

Quantized State Hybrid Automata for Cyber-Physical Systems

Avinash Malik, Partha Roop

Abstract—Cyber-physical systems involve a network of discrete controllers that control physical processes. Examples range from autonomous cars to implantable medical devices, which are highly safety critical. Hybrid Automata (HA) based formal approach is gaining momentum for the specification and validation of CPS. HA combines the model of the plant along with its discrete controller resulting in a piece-wise continuous system with discontinuities. Accurate detection of these discontinuities, using appropriate level crossing detectors, is a key challenge to simulation of CPS based on HA.

Existing techniques employ time discrete numerical integration with bracketing for level crossing detection. These techniques involve back-tracking and are highly non-deterministic and hence error prone. As level crossings happen based on the values of continuous variables, Quantized State System (QSS)-integration may be more suitable. Existing QSS integrators, based on fixed quanta, are also unsuitable for simulating HAs. This is since the quantum selected is not dependent on the HA guard conditions, which are the main cause of discontinuities. Considering this, we propose a new *dynamic* quanta based formal model called Quantized State Hybrid Automata (QSHA). The developed formal model and the associated simulation framework guarantees that (1) all level crossings are accurately detected and (2) the time of the level crossing is also accurate within floating point error bounds. Interestingly, benchmarking results reveal that the proposed simulation technique takes 720, 1.33 and 4.41 times fewer simulation steps compared to standard Quantized State System (QSS)-1, Runge-Kutta (RK)-45, and Differential Algebraic System Solver (DASSL) integration based techniques respectively.

I. INTRODUCTION

Cyber-physical Systems (CPS) combine a set of discrete controllers, the cyber-part of the system, which control a set of physical processes also known as the plant. Such systems are highly safety critical in nature. Consider the example of a nonholonomic robot trying to navigate in an obstacle ridden environment as shown in Figure 1a and obtained from [1].

The solid line shows the trajectory that the robot takes. The robot is moving using rear-wheel drive where v_1 and v_2 are the driving and steering velocities respectively. These values are input by the controller. The position of the robot in the Cartesian plane is denoted by the continuous variables x and y , the steering angle is denoted by ϕ , the orientation of the robot is given by θ and the distance between the front and back wheel is given by the constant l . The robot starts from position $(0, 0)$ and moves towards the end of the room. It is required that the robot should not collide with any of the obstacles. Any collision with an obstacle will lead to the failure of the

robot, which may have safety implications. Considering this, CPS simulation must have formal guarantees.

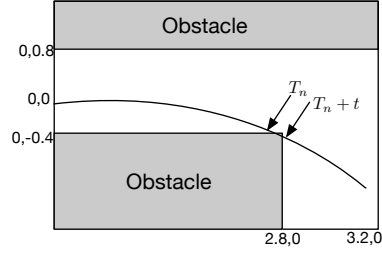
Hybrid Automata (HA) is a formal model, which is widely adopted in the CPS design flow. Formal verification of CPS is ideal for ensuring safety. However, due to well known undecidability result regarding reachability [2], such verification is carried out using restricted subset of HA, such as the recent work using linear HA [3]. This limits the system being modelled and reduces applicability to realistic problems. Consequently, in this paper, we focus on simulation of CPS using HA, so as to guarantee the fidelity of such simulation.

Simulation of HA is also non-trivial. Such an automaton behaves piecewise continuously in every *mode* until a sudden discontinuity happens. Discontinuities are induced when a controller switches the mode of a plant. The controller monitors the plant dynamics and when the plant reaches a pre determined “level”, the controller switches the mode of the plant. This, in turn, changes the behaviour of the plant.

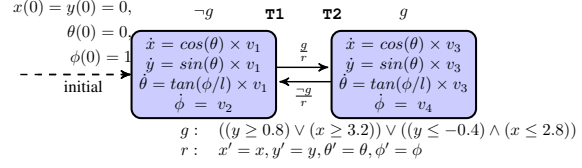
The HA describing the closed-loop dynamics of the robot and the controller is shown in Figure 1b. The robot moves at a constant steering and driving velocities in the obstacle free path, as long as it does not collide with the obstacles. The change in the continuous variables is captured in the location **T1** of the HA. As soon as the robot touches any of the obstacles, the robot stops and changes direction as shown in location **T2** of the HA. Once the robot has steered clear of the obstacles, it goes back to moving at the original steering and driving velocities, as shown by the edge connecting location **T2** to **T1**. The collision with boundaries of the shaded obstacles in Figure 1a is captured by the guard condition g in the HA. The reset relations r highlight the discontinuous updates of the continuous variables.

The most common technique, popularized by tools such as Modelica [4], Simulink and Stateflow [5], [6], for simulation of hybrid systems (including HA) is a two stage process: ① numerical integration of Ordinary Differential Equations (ODEs) followed by ② level crossing detection. The procedure can be described as follows:

- 1) From any given point in time T_n (where $T_n = 0$ for the very first instant) take an integration step t .
- 2) Compute the value of continuous variables at time T_n and $T_n + t$ without committing the integration step.
- 3) Evaluate the guard at time T_n and time $T_n + t$, given the values of the continuous variables computed in point 2 above. If the guard evaluates to true its sign is considered to be positive. Otherwise, it is considered to be negative. If the sign changes, a level crossing has occurred.



(a) The scenario that leads to missed level crossing detection



(b) The HA describing the robot dynamics

Fig. 1: Nonholonomic robot navigation in an obstacle course

- 4) Upon detecting the level crossing, *localization* is performed. Localization determines the most accurate time (within the bounds of floating point error) when the very first level crossing happened by performing a binary search between T_n and $T_n + t$.
- 5) If there is a change in sign, a discrete mode switch is made at the detected time instant and the above steps are repeated.
- 6) If there is no change in sign, the integration step is committed, i.e., all the continuous variable values are advanced to step $T_n + t$ and the above steps are repeated.

For the HA in Figure 1b, the simulation engine took steps such that the robot is just before the obstacle at time T_n and after integration of time step t , it will collide with the obstacle at time $T_n + t$. The guard condition, determining the collision, at time T_n is *false*, because predicate $-0.4 \leq y \leq 0.8$ holds. After a single integration step of size t the guard condition remains *false*, because the predicate $3.2 \leq x \leq 2.8$ holds. Hence, it *appears* that the guard has not changed sign as the simulation engine fails to detect the level crossing. This results in wrong behaviour of the HA, which in turn leads to a safety violation i.e. a collision with the obstacle. For $t = 1.4e^{-4}$, $v1 = 30m/s$, and $v2 = -10m/s$, OpenModelica [7] does not detect the collision with obstacles for the example in Figure 1.

In the general case, any time a HA crosses a level even number of times, the simulation engine may miss the level crossing. Moreover, the engine might detect some other level crossings rather than the first one, which in turn results in incorrect localization. The primary issue is that the step size t of the integrator is chosen independent of the guard conditions. Techniques have been proposed to make the selection of step size sensitive to the guard conditions [8], [9]. However, these approaches are too inefficient in practice, because they require changing the classical numerical integration techniques by incorporating Lie derivatives of the guard set. Furthermore, the most flexible technique [9] cannot handle cases when the ODEs flow tangential to the guard set. To conclude, classical level-crossing detection techniques are unable to correctly handle discontinuities during simulation of network of HAs.

Our major **contribution** in the paper is a quantized state semantics and associated simulation framework for HAs, where sudden discontinuities are correctly captured. Our technical contributions in this paper can be listed as follows:

- 1) A new formal model, called Quantized State Hybrid Automata (QSHA), and its semantics is proposed for the

simulation of CPS.

- 2) A dynamic quantum selection and discrete event simulation technique that converges to the first level crossing is developed. This results in an efficient discrete event simulation engine for QSHA.

The rest of the paper is arranged as follows: Section II describes the preliminary details needed to read the rest of the paper. Section III gives the formal syntax and quantized state semantics of HA and QSHA. Section IV then goes on to describe the discrete event simulation framework. Section V then compares the proposed technique with the current state-of-the-art. We finally conclude in Section VI.

II. PRELIMINARIES — QUANTIZED STATE INTEGRATION WITH LEVEL CROSSING DETECTION

An integration technique that can be more amicable to hybrid system simulation is that of quantizing the state (continuous variables) rather than the time line. This technique is called Quantized State System (QSS) [10], [11], [12], [13]. QSS techniques have been used to model HAs described in the Modelica [4] programming language [14], [15], [16]. QSS based hybrid system simulators also follow the two stage approach: ① integrate ODEs using QSS techniques, and ② perform level crossing detection. Herein we describe the QSS integration approaches, which will be necessary for reading the rest of the paper.

Given a time-invariant ODE system $\dot{x} = f(x(t), t)$, like the ODEs in the locations in Figure 1b, where $x(t) \in \mathbb{R}^n$ is the state vector. QSS approximates the ODE as:

$$\dot{x} = f(q(t), t) \quad (1)$$

where $q(t)$ is the vector containing the quantized state variables, which are quantized version of the state variables $x(t)$.

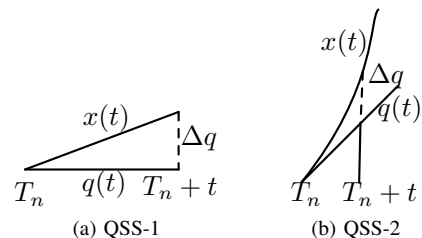


Fig. 2: Quantized State System (QSS) techniques

Each variable $q_i(t)$, $i \in [1, n]$, can be approximated as a piecewise constant, linear, quadratic or any high-order polynomial. We describe the two most common approximations of $q_i(t)$, constant and linear called QSS-1 and QSS-2, respectively.

A. Quantized State System (QSS)-1

The basic premise of first order QSS called QSS-1 is shown in Figure 2a. In case of QSS-1, during integration, of any ODE \dot{x}_i , at any given point T_n (for the very first instant $T_n = 0$), a quantization function $q_i(t)$ is initialised as $q_i(T_n) = x_i(T_n)$. Next, $q_i(t)$ is held constant, i.e., $q_i(t) = q_i(t^-)$, by hysteresis, until some time t , where $x_i(t)$ and $q_i(t)$ diverge by some user specified quantum Δq_i . Formally, we solve a polynomial $|x_i(t) - q_i(t)| = \Delta q_i$ to get the value of t , where $\dot{x}_i = f(q_1(t), \dots, q_i(t), \dots, q_n(t), t)$.

Going back to our running example in Figure 1, for each continuous variable x , y , θ , ϕ , in the system of ODEs in location **T1** in Figure 1b, we initialize the functions $q_x(t)$, $q_y(t)$, $q_\theta(t)$, and $q_\phi(t)$. From the initial conditions in the HA we get $q_x(0) = q_y(0) = q_\theta(0) = 0$ and $q_\phi(0) = 1$, for the very first instant, $T_n = 0$. Similarly, we also have four quanta Δq_x , Δq_y , Δq_θ , and Δq_ϕ for these continuous variables.

For continuous variable x , we have $\dot{x} = f(q_\theta(t), t) = \cos(0) \times v_1 = v_1$, because $q_\theta(t) = q_\theta(t^-) = q_\theta(0) = 0$, by hysteresis. Hence, we solve the polynomial $|\int v_1 d\tau - q_x(t)| = \Delta q_x$. In this case, it is simply $|v_1 \times t| = \Delta q_x$, because $q_x(t) = q_x(t^-) = q_x(0) = 0$ and $x(0) = 0$. In the general case, the integral can be solved using simple explicit Euler technique. Same for all other variables in our system of ODEs. QSS-1 always results in a linear equation (first order polynomial) in t to be solved for its roots.

Once we have the value of variables at time T_n ($T_n = 0$ for the very first instant) and at time $T_n + t$, we can check for the change in the sign of the HA guard to detect level crossing using the technique described in Section I.

B. Quantized State System (QSS)-2

QSS-2 differs from QSS-1 in only the form of the quantized variables. In case of QSS-2, every quantized function $q_i(t)$ is a linear equation, of the form:

$$q_i(t) = q_i(T_n) + \dot{x}_i(T_n) \times (t - T_n)$$

For the very first instant, $T_n = 0$, we have $q_x(0) = q_y(0) = q_\theta(0) = 0$ and $q_\phi(0) = 1$, like before, for the running example. However, this time around, following the linear approximation of quantized variables we get:

$$\begin{aligned} q_x(t) &= 0 + \cos(\theta(0)) \times v_1 \times (t - 0) = v_1 \times t \\ q_y(t) &= 0 + \sin(\theta(0)) \times v_1 \times (t - 0) = 0 \\ q_\theta(t) &= 0 + \tan(\phi(0)/l) \times v_1 \times (t - 0) = \tan(l^{-1}) \times v_1 \times t \\ q_\phi(t) &= 0 + v_2 \times (t - 0) = v_2 \times t \end{aligned}$$

Next, considering, variable x , we have: $\dot{x} = f(q_\theta(t), t) = \cos(\tan(l^{-1}) \times v_1 \times t)$. Hence, we need to solve the equation:

$$\left| \int \cos(\tan(l^{-1}) \times v_1 \times t) d\tau - q_x(t) \right| = \Delta q_x \quad (2)$$

to get t , where $x(t)$ and its quantized form $q_x(t)$ differ by Δq_x , same for other variables in the system of ODEs.

$$\cos(\tan(l^{-1}) \times v_1 \times t) = 1 - \frac{(\tan(l^{-1}) \times v_1 \times t)^2}{2} \quad (3)$$

$$\therefore \left| \int \left(1 - \frac{(\tan(l^{-1}) \times v_1 \times t)^2}{2}\right) d\tau - q_x(t) \right| = \Delta q_x \quad (4)$$

We can approximate the \cos transcendental function by a Taylor polynomial around zero, up to order one, as shown in Equation (3). We get a n -degree polynomial $x(t)$ after integrating the Taylor polynomial (from Equation (4)), using explicit forward Euler. Hence, QSS-2 finds the time step t where the linear equation $q(t)$ and the n -degree polynomial equation $x(t)$ diverge by some user specified quanta as shown in Figure 2b.

QSS has been successfully used in formal frameworks for simulating CPS such as Ptolemy and Modelica [17], [14], [15]. It has also been shown [10] that QSS is faster (in the number of integration steps taken) for some *stiff* systems compared to classical numerical integration techniques like Runge-Kutta. However, note that QSS **like** classical numerical integration uses the same level crossing detection technique. Hence, for any given quantum can also miss level crossing events.

Furthermore, QSS, unlike classical numerical integration, allows integrators to execute asynchronously, which makes combination of QSS integration along with HA ambiguous. Consider the guard condition in the HA in Figure 1b. This guard condition g depends upon two variables x and y , and hence when evaluating the guard, at any point of time T_n or $T_n + t$, value of variables x and y should be available. However, since QSS integrators computing the values of these variables run asynchronously, the values of x and y may *not* be available together at any time instant and hence, the guard cannot be evaluated, leading to incorrect behaviour. Such semantic ambiguities need to be carefully considered.

III. QUANTIZED STATE HYBRID AUTOMATA (QSHA) – SYNTAX AND SEMANTICS

This section formalises the syntax and semantics of QSHA, which uses a new QSS integration technique with HA. We start by defining Hybrid Automata (HA) using Definition 1. When the model comprises of multiple HAs, then the product HA is obtained using an asynchronous cross-product in the standard way [18].

Consider the nonholonomic robot HA shown in Figure 1b for illustration. This HA has two locations and hence $\mathbf{L} = \{\mathbf{T1}, \mathbf{T2}\}$. The continuous variables used in the model are x , y , ϕ , θ i.e., $X = \{x, y, \phi, \theta\}$ and $\mathbf{X} = \mathbb{R}^4$. Location **T1** marked as the initial (or starting) location, hence $Init = \{\mathbf{T1}\} \times \{0\} \times \{0\} \times \{0\} \times \{1\}$. The ODEs, inside the locations, capture the evolution of these continuous variables. Formally, ODEs are represented as vector fields, e.g., $f(\mathbf{T1}, x, t, \phi, \theta) \stackrel{\text{def}}{=} [\dot{x}, \dot{y}, \dot{\phi}, \dot{\theta}]^T = [\cos(\theta) \times v_1, \sin(\theta) \times v_1, \tan(\theta/l) \times v_1, v_2]^T$. Invariants are used as *fairness conditions* to enable an exit from any location

^{1T} indicates transpose of a matrix/vector.

as soon as the invariants become false. They also restrict all continuous variables to obey the invariant conditions, while the execution remains in a given location i.e. the invariant for the location **T2** is $g = ((y \geq 0.8) \vee (x \geq 3.2)) \vee ((y \leq -0.4) \wedge (x \leq 2.8))$. There are two edges $e_1 = (\mathbf{T1}, \mathbf{T2})$, $e_2 = (\mathbf{T2}, \mathbf{T1})$ in E . An example guard on edge e_1 is given by $G(e_1) = g$, which is also the invariant in location **T2**. Similarly, the reset relation on edge e_1 is given as $R(e_1, x, y, \theta, \phi) \stackrel{\text{def}}{=} [x', y', \theta', \phi']^T := [x, y, \theta, \phi]^T$, where x' , y' , θ' , and ϕ' give the updated values of the continuous variables.

Definition 1. A Hybrid Automata (HA) is $\mathcal{H} = \langle L, X, \text{Init}, f, h, \text{Inv}, E, G, R \rangle$, where:

- L a set of discrete locations.
- X is a finite collection of continuous variables, with its domain represented as $\mathbf{X} = \mathbb{R}^n$.
- $\text{Init} \subseteq \{l_0\} \times \mathbf{X}$ such that there is exactly one $l_0 \in L$, is the singleton initial location.
- $f : L \times \mathbf{X} \rightarrow \mathbb{R}^n$ is a vector field.
- $\text{Inv} : L \rightarrow 2^{\mathbf{X}}$ assigns to each $l \in L$ an invariant set.
- $E \subset L \times L$ is a collection of discrete edges.
- $G : E \rightarrow 2^{\mathbf{X}}$ assigns to each $e = (l, l') \in E$ a guard.
- $R : E \times \mathbf{X} \rightarrow \mathbf{X}$ assigns to each $e = (l, l') \in E$, $x \in \mathbf{X}$ a reset relation.

Definition 2. The edge guards G are of the form:

$$g \stackrel{\text{def}}{=} x \bowtie \mathbb{Q} | g \wedge g | g \vee g$$

where $x \in X$ is a continuous variable, $\bowtie \in \{\geq, \leq, >, <\}$, and negation is expressed by reversing the operator in \bowtie .

Definition 3. For a HA $\mathcal{H} = \langle L, X, \text{Init}, f, h, \text{Inv}, E, G, R \rangle$. For some outgoing edge guard $g \in G$, for some edge $e \in E$, let $g = p_1 \wedge p_2$, where $p_1 \stackrel{\text{def}}{=} l_x \bowtie x \bowtie u_x$ and $p_2 \stackrel{\text{def}}{=} l_y \bowtie y \bowtie u_y$, where $\bowtie \in \{<, \leq\}$ and $x, y \in X$ and $l_x, u_x, l_y, u_y \in \mathbb{Q}$. Furthermore, there exists some $t_x^l, t_x^u, t_y^l, t_y^u \in \mathbb{R}$, such that $x(t_x^l) - l_x = 0$, $x(t_x^u) - u_x = 0$, $y(t_y^l) - l_y = 0$, $y(t_y^u) - u_y = 0$ and $\forall t' < t_x^l, x(t_x^l) - l_x \neq 0$, $\forall t' < t_x^u, x(t_x^u) - u_x \neq 0$, $\forall t' < t_y^l, y(t_y^l) - l_y \neq 0$, $\forall t' < t_y^u, y(t_y^u) - u_y \neq 0$. Then, \mathcal{H} is well-formed iff $t_x^l < t_x^l \leq t_x^u \vee t_y^l < t_y^l \leq t_y^u \vee t_x^l = t_y^l$

QSHA is defined using Definition 4.

Definition 4. A Quantized State Hybrid Automata (QSHA) is $\mathcal{H}_q = \langle L, X, X_q, \text{Init}, f, f_q, h, \text{Inv}, E, G, R \rangle$, corresponding to a given HA $\mathcal{H} = \langle L, X, \text{Init}, f, h, \text{Inv}, E, G, R \rangle$. Here for every variable $x \in X$, we introduce a quantised state variable $q \in X_q$. The quantized state version of the vector field f_q is obtained from f as follows: Given any $\dot{x} = f(x(t), t)$, an ODE defined using f , we introduce its quantized state ODE in f_q as follows: $\dot{x} = f(q(t), t)$.

The semantics of QSHA is based on the concept of hybrid timesets with dynamic quanta, hereafter referred to as hybrid timesets, formalised using Definition 5. This semantics uses a dynamic quantum based integration step.

Figure 3 visualises the proposed semantics. Here, time progresses in any location in discrete steps, which is captured as a time interval $I_i^{k_i}$. During this time interval, the QSHA

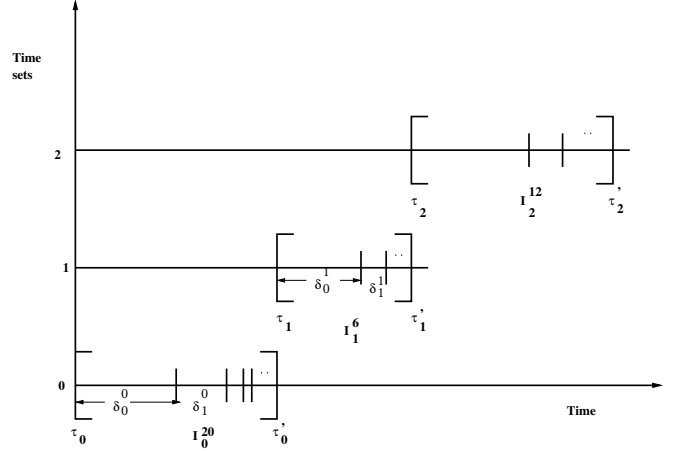


Fig. 3: QSHA semantics

takes k_i discrete steps, where each step corresponds to an integration step of length $\delta_0 \dots \delta_{k_i}$. The duration of each of these integration steps is computed using the algorithm in Section IV. Each of these k_i -steps are known as *intra-location* transitions, as control resides in a given location. Exactly after the passage of k_i -th integration step, an *inter-location* transition is enabled to facilitate an instantaneous location switch. This inter-location transition takes zero time. In Figure 3, three intervals I_0^{20} , I_1^6 and I_2^{12} are visualised. The first interval has 20 sub-intervals of varying lengths indicated by δ_0^0 to δ_{20}^0 , where the time intervals gradually become shorter. Each time interval indicates the duration of an integration step. Informally, the gradually diminishing time intervals make sense, because we are approaching the inter-location transition. A formal reason is provided later in Theorem 2, Section IV-D. Likewise, the next two intervals have 6 and 12, gradually diminishing, integration steps.

Definition 5. A discrete hybrid timeset is a sequence of intervals $\tau = \{I_0^{k_0}, \dots, I_i^{k_i}, \dots, I_n^{k_n}\}$, such that:

- 1) $I_i^{k_i} = [\tau_i = \tau_i^0, \tau_i^1 = \tau_i + \delta_0^i, \dots, \tau_i' = \tau_i + k_i \times \delta_{k_i}^i]$
- 2) If $n < \infty$ then $I_n^{k_n} = [\tau_n = \tau_n^0, \tau_n^1 = \tau_n + \delta_0^n, \dots, \tau_n' = \tau_n + k_n \times \delta_{k_n}^n]$, or $I_n^{k_n} = [\tau_n = \tau_n^0, \tau_n^1 = \tau_n + \delta_0^n, \dots, \tau_n' = \tau_n + k_n \times \delta_{k_n}^n]$, and
- 3) $\tau_i \leq \tau_i'$ and $\tau_i' = \tau_{i+1}$ for all $i < n$.

Remark 1. Given $\tau = \{I_0^{k_0}, I_1^{k_1}, \dots, I_n^{k_n}\}$

- 1) We denote τ as the domain of τ , which includes any time instant t that is in any interval $I_i^{k_i} \in \tau$.
- 2) Each interval $I_i^{k_i}$ has k_i sub-intervals where $(\tau_i' - \tau_i) = \sum_{j=0}^{k_i} \delta_j^i$, and
- 3) For any two consecutive intervals, $I_i^{k_i}$ and $I_{i+1}^{k_{i+1}}$, the ending time of the first interval equals the start time of the second interval i.e. $(\tau_i' = \tau_{i+1})$.
- 4) The instantaneous separation between the time intervals $I_i^{k_i}$ and $I_{i+1}^{k_{i+1}}$ enables instantaneous mode switches. This in turn models infinite state changes in finite time, thereby modelling Zeno artefacts.

The semantics of QSHA is specified as a set of executions. A given execution is defined over a hybrid timeset τ . The execution over τ must satisfy the following three conditions:

① any execution begins in an initial location. ② While executing in a location, a set of intra-location transitions are taken where time progresses in steps of variable length δ . Starting at any given time T_n continuous variables evolve based on the specified ODEs using the variable quantum based integration technique. Moreover, the location invariant must hold. ③ The inter-location transitions are taken when the guard is satisfied and as the transition triggers, some continuous variables are reset according to specified reset relations. This is formalised in Definition 6.

Definition 6. Let Γ be a collection of hybrid timesets. A discrete execution of an QSHA \mathcal{H}_q is a three tuple $\mathcal{X} = (\tau, l, x)$ with $\tau \in \Gamma$, $l : \tau \rightarrow \mathbf{L}$, $x : \tau \rightarrow \mathbf{X}$, satisfying the following:

- 1) *Initial Condition:* $(l(\tau_0), x(\tau_0)) \in \text{Init}$
- 2) *Intra location transitions:* For any interval $I_i^{k_i} = [\tau_i, \tau_i'] \in \tau$ the following must hold:
 - *Invariant satisfaction:* for all $t \in \{\tau_i, \tau_i + \delta_0^i, \dots, \tau_i + k_i \times \delta_{k_i}^i\}$, $x(t) \in \text{Inv}(l(t))$.
 - *Continuous variable updates:* for all $0 \leq j \leq k_i$

$$x(\tau_i) = x(\tau_i^0) \text{ and}$$

$$x(\tau_i^{j+1}) = x(\tau_i^j) + \Delta_x(\delta_j^i), \text{ where } \Delta_x(\delta_j^i) \text{ is a function that selects an appropriate quantum } \Delta_{x_m} \text{ for the continuous variable } x_m, \text{ where } 1 \leq m \leq n, \text{ corresponding to the current integration step of length } \delta_j^i.$$
- 3) *Inter-location transitions:* For all i , $e_i = (l(\tau_i'), l(\tau_{i+1})) \in E$, $x(\tau_i') \in G(e_i)$ and $(x(\tau_{i+1}) \in R(e_i, x(\tau_i'))$.

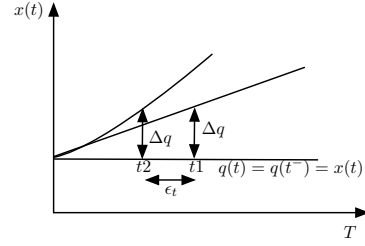
IV. DISCRETE EVENT SIMULATION OF QUANTIZED STATE HYBRID AUTOMATA (QSHA)

Section III fulfils the first objective of the paper, by providing a formal quantized state semantics of QSHA. This section details the discrete event simulation technique, which guarantees that the generated trace adheres to the semantics.

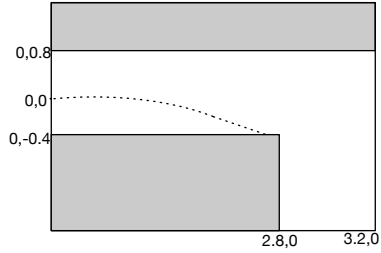
The semantics of QSHA, represented as executions (c.f. Definition 6), captures a set of timed traces of the automaton. Every execution must begin in the initial location l_0 . Execution then progresses from one location to the next when an *inter-location* transition is taken instantaneously following Definition 6, rule 3. When execution begins in a new location, the values of the continuous variables are updated using a set of $\delta_0^i, \dots, \delta_{k_i}^i$ steps of gradually diminishing integration steps in the interval $I_i^{k_i}$. These are known as intra-location transitions following Definition 6, rule 2. The duration of integration steps are decided using a new QSS algorithm based on dynamic quanta, we term DQSS, which is elaborated next.

A. Computing the next scheduling event for each continuous variable

Algorithms 1 provides the pseudocode for computing a time instant when the next integration step is scheduled. The presented technique leverages QSS-1 and a revised version of QSS-2 integration techniques. Figure 4 visualises the key idea of the proposed integration technique. Based on a given level crossing value for a continuous variable x , we select an initial guess of the level crossing as the $\Delta q = \mathbf{L}_x - x$



(a) The primary idea for finding the next time event using a dynamic quanta obtained from the level crossing



(b) The output trace for nonholonomic robot from the proposed technique. The trace always converges to the level-crossing, but never crosses it like in other techniques.

Fig. 4: Dynamic quantum selection and scheduling event generation

```

Input : Ode
Input : currentValues
Input : levelCrossings
// The next time event t to schedule QSHA
Output:  $\mathbb{R}$ 
1 if 0  $\in$  levelCrossings then
2   return 0
3 else
4   foreach  $l \in$  levelCrossings do
5      $toRet \leftarrow toRet \cup \{DQSS(Ode, currentValues, l)\};$ 
6   end
7 end
// Return the very first integration step
8 return  $\min(toRet)$ 

```

Algorithm 1: The nextEvent algorithm

where \mathbf{L}_x is the value of the level crossing. Usually \mathbf{L}_x is the value of the continuous variable x that satisfies one or more of the outgoing edge guard condition from any location of the HA. Furthermore, x is the current value of x . We then perform QSS-1 integration to compute the time instant (discrete event) $t1$ where $x(t) - q(t) = \Delta_q$, where $q(t)$ is held constant using hysteresis. We also compute a time instant $t2$ where $x(t) - q(t) = \Delta_q$ where $q(t)$ is computed using a linear approximation while $q(t)$ is held constant like before (this is a variant of QSS-2). If $t2 - t1 > \epsilon_t$ then the selected quantum Δ_q is too large as the error in the QSS-1 approximation is too large. We then halve the quantum and repeat the above steps until the required error bound is achieved. Algorithm 2, which performs the above tasks recursively, is called by nextEvent algorithm described below.

The nextEvent algorithm (Algorithm 1) takes as input three arguments: ① The ODE of the continuous variable being used to compute the scheduling event, ② the current values of all continuous variables in the QSHA, and ③ a list of level crossings for this continuous variable. For example, in location T1, in Figure 1b, the variable x has two possible

```

1 DQSS(Ode, currentVals, quanta)
  // Compute t1 using QSS-1 Section II-A
2 t1 ← QSS1(Ode, currentVals, quanta);
  // Compute t2 using  $\Delta q = n$  degree polynomial  $q(t) - q(t)^-$ 
3 t2 ← MQSS2(Ode, currentVals, quanta);
  // If  $t1 - t2 < \epsilon_t$  then return the value of t1
  // Dynamic selection of  $\Delta q$ 
4 if  $abs(t1 - t2) < \epsilon_t$  then
5   return t1
6 else
7   return DQSS(Ode, currentVals, quanta/2)
8 end

```

Algorithm 2: The DQSS algorithm, computing the next time event t

values, 3.2 and 2.8, that can satisfy guard g . Hence, the input levelCrossings is the vector $[3.2 - x, 2.8 - x]$, where x is the current value of the continuous variable x . The algorithm returns a single real number, which represents the future time event when the QSHA maybe executed.

Algorithm 1 first checks if any of the level crossings has already happened (line 2). If a level crossing has already happened, the QSHA is expected to be scheduled right this instant and hence, the future integration step of 0 is returned.

If the level crossing has not yet occurred, then the Dynamic Quantized State System (DQSS) (Algorithm 2) is called to determine the next time event to schedule the QSHA for *each* level in the levelCrossings input (lines 4-5). Notice that the last argument of Algorithm 2 is the quanta (line 1), which is set to the level crossing of the variable (line 5, Algorithm 1), when called from Algorithm 1. The *minimum* from amongst all the returned values from Algorithm 2 (line 8) is returned for scheduling the QSHA.

B. Simulation of QSHA

Algorithm 3 describes the top-level discrete event simulation engine for simulating the QSHA. The algorithm takes as input the QSHA that needs to be simulated (\mathcal{H}_q) and the total time for simulation (U) and produces the output trace Γ . The algorithm starts by declaring two counters (T_n and T_{pre}) for holding the current instant of execution and previous instant of execution of \mathcal{H}_q respectively. Variable t represents the duration of the discrete event simulation step. Variables X_{now} and X_{pre} represent the values of the continuous variables of the QSHA at time T_n and T_{pre} respectively. Variable *enable* holds the current enabled location of \mathcal{H}_q , which is initialized to the initial location l_0 at the start of simulation i.e. $T_n = 0$.

Algorithm 3 starts by initializing all the variables in dictionary X_{pre} with the initial values specified by *Init* of the QSHA (line 1). For the nonholonomic robot running example (Figure 1b), line 1 in the algorithm would initialise $x = y = \theta = 0$ and $\phi = 1$ in the set X_{pre} . The output trace Γ is always concatenated with the values of the variables from X_{pre} along with the current time T_n and the enabled location (line 18).

The main simulation engine is a loop that iterates, executing the QSHA in discrete time steps until the current simulation time is less than or equal to the total user specified simulation time (line 2). The execution of the QSHA is carried out as follows:

```

Input : QSHA  $\mathcal{H}_q = \langle L, X, X_q, Init, f, f_q, h, Inv, E, G, R \rangle$ 
Input : Simulate until time  $U$ 
Output: Trace  $\Gamma$ 
// Current simulation time
Data:  $T_n \leftarrow 0$ 
// Previous value of  $T_n$ 
Data:  $T_{pre} \leftarrow 0$ 
/* The next event time */
Data:  $t \leftarrow 0$ 
// Previous value of continuous variables
Data:  $X_{pre} \leftarrow \{0|x \in X\}$ 
// Current value of continuous variables
Data:  $X_{now} \leftarrow \{0|x \in X\}$ 
/* Location enabled for execution */
Data:  $enable \leftarrow l_0$ 
/* Initialise the pre-form variables */
1  $X_{pre} \leftarrow \{x|(enable, x) \in Init\}$ 
/* While simulation time has not exceeded time  $U$  */
2 while  $T_n \leq U$  do
  // For each enabled location
  3 TOP: for  $l \in L \wedge enable == l$  do
    /* All outgoing edges of location  $l$  */
    4 foreach  $e \in E \wedge e(0) == l$  do
      /* pre variables satisfy guard ---
      inter-location transition */
      5  $\hat{X}_{pre} = \{X_{pre} \in 2^{X_{pre}} | X_{pre} \subseteq G(e)\};$ 
      6 if  $X_{pre} \neq \emptyset$  then
        7  $X_{now} \leftarrow \{x|x \in R(e, X_{pre})\}$ 
        /* Update the next enabled location */
        8  $enable \leftarrow e(1);$ 
        /* location switch is instantaneous and
        hence  $t$  is set to 0 */
        9  $t \leftarrow 0;$ 
        /* Jump out of loop */
        10 break TOP;
      end
    end
    11 end
    /* Evolve ODEs in location  $l$  using Euler
    integration--- intra-location transition */
    // For the very first time,  $T_n = T_{pre} = 0$ 
    13  $\delta \leftarrow T_n - T_{pre};$ 
    14  $X_{now} \leftarrow X_{pre} + f(l, X_{pre}) \times \delta;$ 
    /* Compute next discrete event  $t$  */
    15  $t \leftarrow compute\_next\_event(\mathcal{H}_q, l, X_{now});$ 
    16 end
    /* Update the pre variables */
    17  $X_{pre} \leftarrow X_{now};$ 
    /* Concatenate to output trace */
    18  $\Gamma \leftarrow \Gamma \cup \{(T_n, enable, X_{pre})\};$ 
    /* Save current time  $T_n$  */
    19  $T_{pre} \leftarrow T_n;$ 
    /* Increment the simulation time by  $t$  */
    20  $T_n \leftarrow T_n + t;$ 
  21 end
22 return  $\Gamma$ 

```

Algorithm 3: Top-level Discrete Event Simulation engine for QSHA

- 1) From any enabled location, first the guards on all outgoing edges are checked. If any guard is **True**, then the outgoing edge is taken instantaneously in zero simulation time. This behaviour corresponds to the inter-location transition described in Section III and implemented from lines 4-11 in Algorithm 3. For the running example of the nonholonomic robot in Figure 1b, location **T1** is selected by line 3 as being enabled initially. Next, the loop body (lines 5 and 6) checks if the values in X_{pre} satisfy the outgoing edge guard g from Figure 1b. If the guard condition is satisfied, then the variables X_{now} are updated according to the reset relation on the outgoing edge (line 7). Finally, the next destination location is enabled (line 8), the next event variable t is set to zero (line 9) and the algorithm iterates after updating the pre set of variables, the current simulation timer, and the output trace (lines 10 and 17-20).

2) If none of the outgoing edge guards hold then, ④ the ODEs in the enabled location of a QSHA evolve (lines 13 and 14) and ⑤ the *future* discrete time event t , when the QSHA will be executed next is computed (line 15) — this behaviour corresponds to the intra-location transition described in Section III. During evolution of the ODE and computation of the future discrete event t the following actions are performed:

- a) The values of the continuous variables are updated using the standard forward Euler numerical integration technique. This integration uses the values from X_{pre} and the updates are performed on the variables of X_{now} , i.e., the right hand-side of all updates work on the variables from the X_{pre} , while the left hand side updates are always performed on the X_{now} . In case of the running example, the nonholonomic robot, this step would evolve the variables x , y , θ , and ϕ in location **T1** or **T2**. The very first iteration of the algorithm, which evolves the ODEs has a time step (δ) of zero (line 13), because for the very first time $T_n = T_{pre} = 0$. Thus, the variables will not change their values at the start, until the duration of non-zero integration step is decided (see below).
- b) The calculation of the future discrete simulation event t is carried out by function `compute_next_event` described in Algorithm 4. This function takes as input the QSHA (\mathcal{H}_q), the current enabled location l , and X_{now} , which contains the current values of the continuous variables. This next discrete time event t returned by this function is used to schedule the QSHA in the next iteration of the algorithm. The `compute_next_event` function is described in the next section.

C. Computing the next discrete simulation (integration) step

```

Input : QSHA  $\mathcal{H}_q = \langle L, X, X_q, Init, f, f_q, h, Inv, E, G, R \rangle$ 
// The current enabled location
Input :  $enabled \in L$ 
// The current value of continuous variables
Input :  $X_{now}$ 
// The next discrete simulation/integration event  $t$ 
Output:  $t : \mathbb{R}^{\geq 0}$ 
// Initialize set  $\tilde{ts}$ 
1  $\tilde{ts} \leftarrow \emptyset$ ;
2 foreach  $e \in E \wedge e(0) == enabled$  do
    /*  $LC$  is a  $M \times |X|$  matrix, where each row indicates
       the value of continuous variables that satisfy
       the outgoing edge  $e$  guard  $G(e)$  */
3    $LC \leftarrow [\mathbb{R}^{|X|} | \forall R^{|X|} \in 2^{\mathbb{R}^{|X|}} \wedge R^{|X|} \subseteq G(e)];$ 
4   foreach  $x \in X$  do
5      $ode_x \leftarrow f_q(l, X_{now}[x]);$ 
    // Index through each column in  $LC$ 
6      $LC_x \leftarrow \{ \mathbb{R} - X_{now}[x] | \mathbb{R} \in LC^T[x] \};$ 
    /* If guards depends upon  $x$  */
7     if  $LC_x \neq \infty$  then
8        $\tilde{ts} \leftarrow \tilde{ts} \cup \{ \text{nextEvent}(ode_x, X_{now}, LC_x) \};$ 
9     end
10  end
11   $t \leftarrow \min(\tilde{ts});$ 
12  return  $t$ 
13 end
```

Algorithm 4: Function `compute_next_event` that computes the next discrete simulation/integration step event

Algorithm 4 describes the function that computes the next discrete simulation/integration step. This function takes as

input the QSHA \mathcal{H}_q , the currently enabled location $enabled$, and the current valuation of the continuous variables X_{now} . The function returns a real value t , which indicates the next integration and discrete event simulation step.

Algorithm 4 first initializes a set \tilde{ts} (line 1), which will hold the future event for each variable used in the guard g of the outgoing edge of the currently enabled location. In case of the nonholonomic robot, two variables x and y are used in the guard g from location **T1**. Hence, the set \tilde{ts} will hold two future time events. Next, the algorithm computes the matrix LC , which satisfies the guard on each outgoing edge of the enabled location (line 3). In case of the nonholonomic robot, with **T1** as the enabled location, with a single outgoing edge, the matrix LC is given by Equation (5). The columns in Equation (5), represent x , y , θ , and ϕ , respectively. Notice that \mathbb{R} denotes that the guard is satisfied for any value of that variable, i.e., the guard is *not* affected by that variable.

$$LC = \begin{bmatrix} x & y & \theta & \phi \\ 3.2 & 0.8 & \mathbb{R} & \mathbb{R} \\ 2.8 & -0.4 & \mathbb{R} & \mathbb{R} \end{bmatrix} \quad (5)$$

Finally, for each continuous variable, if the guard on the outgoing edge depends upon that variable, the `nextEvent` function calculates the future discrete event to schedule the QSHA (lines 4-16). In case of the nonholonomic robot, the set \tilde{ts} contains two possible real values when the QSHA can be scheduled, because the guard only depends upon variables x and y . The last argument (LC_x) to function `nextEvent`, is a vector of real values indicating the *difference* between the values of variables that satisfy the guard and the current value of the continuous variables. For example, when calling `nextEvent` for variable x $LC_x = [3.2 - x, 2.8 - x]$, where x indicates the current value of variable x . The algorithm returns the minimum from amongst all the values in \tilde{ts} for scheduling the QSHA.

D. Properties of the proposed dynamic quantum based simulation

There are a number of useful properties that the proposed DQSS simulation technique enforces.

a) *Simulation progress:* As described in Section IV-A, we find two time instants $t1$ and $t2$, for QSS-1 and revised QSS-2, when selecting the quantum Δq dynamically. These time instants are roots of polynomials of some degree n . In case of the running example, for instance, solving QSS-1 results in a linear equation (polynomial of degree 1, c.f. Section II-A), while QSS-2 results in a polynomial with a transcendental function (c.f. Equation (2) c.f. Section II-B). This transcendental function needs to be expanded to a Taylor series, with finite terms, resulting in a polynomial of degree n . The roots of these polynomials are the discrete time events when the QSHA can be scheduled. Our technique always results in at least one real positive root for the n degree polynomial (Equation (4)), which we prove in Theorem 1². This property guarantees that simulation always makes progress.

²This property is not guaranteed for standard QSS-2 and higher degree QSS techniques

Theorem 1. Let $f(x) = a_n x^n + a_{n-1} x^{n-1} + \dots + ax \pm \Delta q = 0$, be a polynomial of degree n with real coefficients. Then $f(x)$ has at least one real positive root.

Proof. Let $v = n - l$, $\forall l \in [1, n]$ be the number of sign changes of the sequence (a_n, \dots, a) . Then by Descartes's rule of signs [19] we have $p = v - 2m$, where p is the number of real positive roots for some non-negative integer m , i.e., $m \in \mathbb{Z}^{\geq 0}$. From fundamental theorem of algebra we have $p \geq 0$. Thus, if a polynomial has no real positive roots, $p = 0$. This can happen only when $m = \frac{v}{2} = \frac{n-l}{2}$, for polynomial with coefficients (a_n, \dots, a) .

Case 1: $n - l$ is an even number. We can always make it an odd number by adding Δq , which has the opposite sign to that of coefficient a . Hence, for polynomial $f(x)$, we get $m = \frac{(n-l+1)}{2}$ if there are no real positive roots. But, $n - l + 1$ is odd, because $n - l$ is even. Thus, $m \notin \mathbb{Z}^{\geq 0}$, which violates Descartes's rule. The value that m can take for minimum p , such that $p \geq 0$ and $m \in \mathbb{Z}^{\geq 0}$ is one less than $\frac{(n-l+1)}{2}$, which is $\frac{n-l}{2}$. Hence, $p = n - l + 1 - (2(\frac{n-l}{2})) = 1$. Hence, there is at least one real positive root of the polynomial $f(x)$.

Case 2: $n - l$ is an odd number. We can enforce that $n - l$ remains odd, by adding Δq with the same sign as that of coefficient a . Hence, for polynomial $f(x)$ to have zero real positive roots, we have $m = \frac{n-l}{2}$. Here again, since $n - l$ is odd, $m \notin \mathbb{Z}^{\geq 0}$. The value that m can take for minimum p , such that $p \geq 0$ and $m \in \mathbb{Z}^{\geq 0}$ is $\frac{(n-l-1)}{2}$. Giving us $p = n - l - (2(\frac{n-l-1}{2})) = 1$. Hence once again there is at least one real positive root of the polynomial $f(x)$. ■

b) *The simulation always detects the first level crossing:* Algorithm 3 line 13 uses forward Euler to evolve the ODEs using the time-step returned by QSS-1 (Algorithm 2 line 5). First we show that this is correct, i.e., from any given point in time T_n if we use forward Euler to compute the integral $(x(T_n+t))$ of any function $x(t)$, where time-step t is computed using QSS-1 with a quantum Δq , then $|x(T_n+t) - x(T_n)| = \Delta q$.

Lemma 1. For some function $x(t)$, let $\dot{x} = f(x(t), t)$ be its slope. Then, given $x(T_n+t) = \dot{x} \times t + x(T_n)$ by forward Euler, where t is obtained by QSS-1 for function $x(t)$ using a quantum of Δq , $|x(T_n+t) - x(T_n)| = \Delta q$.

Proof. Simplifying our goal, we have:

$$x(T_n+t) = \pm \Delta q + x(T_n) \quad (6)$$

$$\therefore f(x(T_n), T_n) \times t + x(T_n) = \pm \Delta q + x(T_n) \quad (7)$$

$$\therefore f(x(T_n), T_n) = \pm \Delta q / t \quad (8)$$

By definition of QSS we have:

$$\dot{x} = f(q(t), t) \quad (9)$$

Integrating $x(t)$ using forward Euler from T_n to t with the QSS approximation we have:

$$x(T_n+t) = f(q(t), t) \times t + x(T_n) \quad (10)$$

By hysteresis in QSS-1 we have:

$$q(t) = q(t^-) = x(T_n) \quad (11)$$

$$\therefore x(T_n+t) = f(x(T_n), T_n) \times t + x(T_n) \quad (12)$$

By QSS-1, we have

$$x(T_n+t) - q(t) = \pm \Delta q \quad (13)$$

$$\therefore \text{by hysteresis } x(T_n+t) - x(T_n) = \pm \Delta q \quad (14)$$

$$\therefore f(x(T_n), t) \times t + x(T_n) - x(T_n) = \pm \Delta q \quad (15)$$

$$\therefore t = \pm \Delta q / f(x(T_n), t) \quad (16)$$

Substituting Equation 16 in Equation 8 we have

$$f(x(T_n), T_n) = \pm \Delta q / (\pm \Delta q / f(x(T_n), T_n)) \quad (17)$$

$$\therefore f(x(T_n), T_n) = f(x(T_n), T_n) \quad (18)$$

■

Theorems 2 and 3 together show that Algorithm 3 always converges to the first level crossing from any given location in the QSHA.

Theorem 2. Given a QSHA $\mathcal{H}_q = \langle L, X, X_q, \text{Init}, f, f_q, h, \text{Inv}, E, G, R \rangle$, $\exists t \in \mathbb{R}$, such that $x(t) \in G(e), \forall e \in E, \forall x \in X_q$ and $\forall T_n \in [0, t)$, $x(T_n) \notin G(e), \forall e \in E, \forall x \in X_q$. Then, in any given location $l \in L$, $\int_{T_n}^{T_n+\delta} \dot{x}(\tau) d\tau \in G(e), \forall x \in X$, i.e., our simulation technique can take an integration step δ , such that the level crossing is satisfied and $T_n + \delta = t$.

Proof. Without loss of generality we consider each continuous variable $x \in X_q$ separately. Note that our integration technique always returns the next time event τ_1 , which corresponds to the QSS-1 integration step (Algorithm 2, line 5). Hence, we apply the definition of QSS-1 (c.f. Section II-A) to prove this theorem. From QSS-1, we have:

$$|x(T_n+\delta) - q(T_n)| = \Delta q \quad (19)$$

$$\therefore |x(T_n+\delta) - x(T_n)| = \Delta q, \text{ by hysteresis} \quad (20)$$

$$\therefore x(T_n+\delta) - x(T_n) = \pm \Delta q \quad (21)$$

From Algorithms 1 and 2, our simulation technique selects a $\Delta q \leq x(t) - x(T_n)$.

Case 1: $\Delta q = x(t) - x(T_n)$. By forward Euler $x(T_n+\delta) = \delta \times \dot{x}(T_n) + x(T_n)$. Applying Equation (20), we have

$$\delta \times \dot{x}(T_n) + x(T_n) - x(T_n) = \pm \Delta q \quad (22)$$

$$\therefore \delta = \pm \frac{\Delta q}{\dot{x}(T_n)} \quad (23)$$

We choose a positive or negative Δq , such that δ is always real positive (from Theorem 1). Hence, in this case, assuming $\dot{x}(T_n)$ is positive, without loss of generality, and choosing a positive Δq , and substituting δ back in forward Euler, we have:

$$x(T_n+\delta) = x(T_n) + \frac{\Delta q}{\dot{x}(T_n)} \times \dot{x}(T_n) \quad (24)$$

$$\therefore x(T_n+\delta) = x(T_n) + \Delta q \quad (25)$$

$$\therefore x(T_n+\delta) = x(T_n) + x(t) - x(T_n) \quad (26)$$

$$\therefore x(T_n+\delta) = x(t) \quad (27)$$

Hence, $x(T_n + \delta) \in G(e)$ and by injective property of functions $T_n + \delta = t$.

Case 2: $\Delta q < x(t) - x(T_n)$. From Equation (23), we have some $\delta' < \delta$, where δ is given by Case 1. Hence, $T_n + \delta' < T_n + \delta$. Binding T_n to $T_n + \delta'$, we need to prove that $\int_{T_n}^{T_n + \delta'} \dot{x}(\tau) d\tau \in G(e)$, which can be proven recursively from Case 1 and Case 2. ■

From Equation (23) it is clear that the discrete integration (simulation) step size δ is directly proportional to the selected quantum Δq . As the current values ($x(T_n)$) of the continuous variables get closer to the level crossings, i.e., values that satisfy the outgoing edge guards ($x(t)$), Δq becomes smaller, because $\Delta q \leq x(t) - x(T_n)$. Consequently, the integration step size also becomes smaller as we approach the level crossings, which is as shown in Figure 3.

Theorem 3. *Given a well-formed HA and consequently a well-formed QSHA $\mathcal{H}_q = \langle L, X, X_q, Init, f, f_q, h, Inv, E, G, R \rangle$ Algorithm 3 always converges to a time event t , such that $\forall x \in X, x(t)$ satisfies $G(e)$ and $\forall t' < t, x(t')$ does not satisfy $G(e), \forall e \in E$.*

Proof. We will consider the case where the guard for any edge $e \in E$ is only dependent upon two variables $x, y \in X$, and the proof can be generalized to any number of variables.

Case 1: We consider the case where the guard is a disjunction of two variables x and y of the form: $l_x \bowtie x \bowtie u_x \vee l_y \bowtie y \bowtie u_y$, where $\bowtie \in \{<, \leq\}$. We need to show that Algorithm 3 always finds the time instant t such that $x(t) \in [l_x, u_x] \vee y(t) \in [l_y, u_y]$ and $\forall t' \in [0, t)$ the guard is not satisfied.

Case a: There exists some $t_x^l < t_y^l$ such that $x(t_x^l) - l_x = 0$ and $\forall t' \in [0, t_x), x(t') - l_x \neq 0$, from Theorem 2, where t_y^l is the first time instant where $y(t_y^l) - l_y = 0$ again from Theorem 2. Hence, $x(t_x^l) \in [l_x, u_x]$. By definition of disjunction $x(t_x^l) \in [l_x, u_x] \vee y(t_x^l) \in [l_y, u_y]$. Algorithm 3 always selects the minimum from amongst all the times for each variable (line 11). Hence, it satisfies the requirement $t_x^l < t_y^l$.

Algorithm 3 always finds the time $t = t_x^l = t_y^l$ and $t = t_y^l$ s.t., $t_y^l < t_x^l$ when the outgoing edge guard holds follows the same reasoning as case a.

Case 2: We consider the case where the guard is a conjunction of two variables x and y of the form: $l_x \bowtie x \bowtie u_x \wedge l_y \bowtie y \bowtie u_y$, where $\bowtie \in \{<, \leq\}$. We need to show that Algorithm 3 always finds the time instant t such that $x(t) \in [l_x, u_x] \wedge y(t) \in [l_y, u_y]$ and $\forall t' \in [0, t)$ the guard is not satisfied.

Case a: There exists $t_x^l < t_y^l$ such that $x(t_x^l) - l_x = 0$ and $\forall t' \in [0, t_x), x(t') - l_x \neq 0$, from Theorem 2, where t_y^l is the first time instant where $y(t_y^l) - l_y = 0$ again from Theorem 2. Let t_x^u be the first time instant where $x(t_x^u) - u_x = 0$ from Theorem 2. If $t_x^l < t_y^l \leq t_x^u$, then the first time instant t where the conjunctive guard is satisfied is $[t_x^l, t_x^u] \cap \{t_y^l\} = t_y^l$. Since Algorithm 3 selects the minimum time from amongst level crossing times for all variables (line 11), it always finds time

TABLE I: Benchmark description

Benchmarks	#L	#ODEs	ODE types	Level-crossing interval	Simulation Time (sec).
TH	2	2	Linear	Open	0.5
WLM	4	8	Linear	Open	30
Robot	2	8	Non-Linear	Open, logically combined	0.07
AFb	4	20	Non-Linear	Open	1.6
Reactor	4	9	Linear	Closed, logically combined	30

$t = t_y^l$. Case $t_y^l > t_x^u$ cannot happen, because then the QSHA is not well-formed.

Algorithm 3 finds the time instant $t = t_x^l = t_y^l$ and $t = t_y^l$ s.t., $t_y^l < t_x^l$ follows the same reasoning as case a. ■

Figure 4b gives the resultant trace of the nonholonomic robot. Notice that the QSHA always converges to the level crossing, i.e., the obstacle, but never overshoots it.

V. EXPERIMENTAL RESULTS

This section describes the experimental set-up and results that we use to quantitatively validate the proposed discrete event simulation technique for QSHA.

A. Benchmark description

We have selected a number of different published benchmarks from different domains and complexity to validate the proposed technique. A quick overview of the selected benchmarks is provided in Table I. These HAs are converted into QSHAs before simulation. We give a more detailed overview of the benchmarks here in:

- **Thermostat (TH):** The TH [20] benchmark is a HA with two locations (indicated by #L in Table I) with one ODE in each location. TH benchmark describes maintaining the temperature in a room between an upper and lower bound. The ODEs are linear, of the form $\dot{x} = f(x(t), t)$. The guards on HA' edges (level crossings) are open intervals, e.g., $x \geq \theta$ or $x \leq \theta$. After 0.5 seconds of simulation time the HA reaches a steady state with a repeating trace.
- **Water Level Monitor (WLM):** The WLM [21] example is a HA that maintains the water in tanks within some level. This HA contains four locations (indicated by #L in Table I) with two ODEs in each location. The ODEs have a constant slope. The edge guards (level crossings) are open intervals like in TH. After 30 seconds of simulation time, the HA reaches a steady state with a repeating trace.
- **Nonholonomic Robot (Robot):** The Robot [1] example is the running example from the paper. As seen from Figure 1b, there are two locations with 8 ODEs altogether. The ODEs in this example are non-linear. In fact, the slopes are transcendental (trigonometric) functions, which are *approximated* with a Taylor polynomial. The guards on HA' edges are open intervals, but dependent upon more than one variable. For example, the guard g in Figure 1b depends upon two variables x and y . We

TABLE II: Tool set-up

Technique	Δq	ϵ_v	ϵ_t	maximum Δt
QSS-1	10^{-3}	10^{-6}	N/A	N/A
RK-45	N/A	10^{-6}	N/A	1.0
DASSL	N/A	10^{-6}	N/A	Sim Time/500
Proposed Tech.	Dynamic	0	10^{-3}	N/A

detect a collision with the objects within 0.07 simulation seconds when $v_1 = 30$ m/s and $v_2 = -10$ m/s in Figure 1b.

- Atrial Fibrillation (AFb): The AFb [22] HA simulates fibrillation (abnormal heart rhythm) in the human atria. There are a total of four locations with five ODEs in each location. The ODEs are coupled and complex of the form:

$$\begin{aligned}\dot{u} &= e + (u - \theta_v)(u_u - u)vg_{fi} + wsg_{si} - g_{so}(u) \\ \dot{s} &= \frac{g_{s2}}{(1 + \exp(-2k(u - us)))} - g_{s2}s \\ \dot{v} &= -g_v^+ \cdot v \\ \dot{w} &= -g_w^+ \cdot w\end{aligned}$$

In the above equations u indicates the transmembrane potential of the heart, v is the fast channel gate, while w and s are slow channel gates for sodium, potassium, and calcium ionic flow. The rest are constant parameters. Once again the exponential function is *approximated* with a Taylor polynomial. AFb reaches a Zeno state after 1.6 seconds of simulation time.

- Nuclear Reactor (Reactor): Reactor [23] HA simulates cooling and control of a nuclear plant. It contains four locations, three of which have three ODEs each and the fourth location is a shut-down location. An interesting aspect of this benchmark is that the edge guards have closed interval of the form $x = y \wedge \tau = \theta^3$, i.e., there are equality constraints combined together with conjunction. Equality on level crossings is known to be difficult to deal with in most hybrid simulation frameworks. Furthermore this HA is also *non-deterministic*. We purposely chose this example to see how the other discrete event simulation tools handle both equality on edge guards and non-determinism. The Reactor in this benchmark shuts-down after 30 seconds of simulation time.

B. Tool set-up

We have compared the proposed discrete event simulation framework, available from [24], with Ptolemy [25], which is a robust discrete event simulation framework for different design paradigms, including HA. Ptolemy allows simulating HAs with QSS [17] and Runge-Kutta techniques. We also used Modelica [4] programming language and the OpenModelica [7] simulation framework for comparison purposes.

The configuration of the tools in listed in Table II. In Table II, Δq is the absolute quantum, ϵ_v is the error tolerance of the values computed from integrators. QSS, RK-45 and DASSL techniques also use the ϵ_v in their level crossing detection algorithms. Parameter ϵ_t is the error tolerance in the

TABLE III: Number of simulation steps taken by different techniques. MLC: Missed Level Crossing.

Benchmarks	Ptolemy-QSS-1	Ptolemy-RK-45	Open-Modelica-DASSL	Proposed Tech.
TH	3361	38	78	54
WLM	38000	61	252	19
Robot	1662	13	MLC	41
AFb	3170	41	151	36
Reactor	72503	68	MLC	15

time domain, when finding roots of polynomials, needed for the proposed technique. Finally, maximum Δt is the maximum integration step that fourth-fifth order RK-45 and DASSL integration techniques can take. The maximum Δt value in Table II is the default value used by the respective tools. In addition to the above set-up, the proposed technique uses five terms in the Taylor polynomials when approximating the transcendental functions.

We would like to point out that only QSS-1 gave correct results in Ptolemy, and hence we compare with only QSS-1. Furthermore, QSS integration does not interact well with HA semantics. The advantage of QSS, i.e., integrators running asynchronously to each other, becomes a hindrance in correct execution of the HA. Consider the Robot HA in Figure 1b. In order to detect that the guard g on the edge connecting **T1** and **T2** is enabled, the value of continuous variables x and y should be available at the same time. However, due to the asynchronous nature of the QSS integrators these values are *not* available in the same time instant. Hence, the guard never triggers and the level crossing is missed, resulting in incorrect behaviour. We enforced synchronous execution of all the QSS integrators by triggering every integrator when any one integrator produces an output.

C. Results

We present two sets of results: ① execution time in terms of the number of discrete simulation steps taken by each of the simulation tool. ② Correctness of the proposed technique by comparing the output traces.

1) *Execution time*: Table III gives the number of steps taken by each of the simulation tool. We compare in terms of simulation steps like [10]. One cannot directly compare the absolute execution time, because each tool is implemented using different programming languages and libraries, Ptolemy in Java, OpenModelica in C++ and the proposed technique in Python.

Out of the five benchmarks, OpenModelica was able to simulate the least number of benchmarks correctly. For our benchmarks, on average, the proposed technique takes $\approx 720 \times$ fewer steps than QSS-1, $1.33 \times$ fewer steps than RK-45 solver and around $4.41 \times$ fewer steps than OpenModelica with the DASSL solver. The proposed technique and Ptolemy's level crossing detector were able to handle equality on edge guards, for the Reactor benchmark, correctly. OpenModelica on the other hand resulted in missed level crossing detections (indicated as MLC in Table III). The proposed technique is correctly able to handle equality, because, unlike other techniques, simulation always converges towards the first level

³Equality can be expressed using less than or equal to operators from Definition 2

TABLE IV: Correlation Coefficients. Ideal value is 1.0

Benchmarks	Ptolemy-QSS-1	Ptolemy-RK-45	Open-Modelica-DASSL
TH	0.999986	1.0	1.0
WLM	1.0	0.865148	1.0
Robot	1.0	1.0	N/A
AFb	0.999861	0.999409	0.999999
Reactor	1.0	1.0	N/A

crossing and never overshoots it as shown in Theorems 2 and 3.

In our simulation framework the non-deterministic Reactor HA is converted into a deterministic HA, by *always* choosing the *same* outgoing edge, from any given state, when more than one outgoing edge are enabled. In case of Ptolemy one of the outgoing edge is chosen randomly during program execution [25].

2) *Correctness of the proposed technique*: Closed form solutions are not possible for all ODEs in our benchmarks, e.g., the ODEs in the AFb benchmark have no closed form solutions. We compare the output trace from the proposed technique with output traces of other techniques to validate the soundness of the proposed approach. Given an output trace, for any benchmark, we obtain the discrete time events, during simulation, when the level-crossing was detected. We correlate these discrete time instants from the proposed technique with QSS-1, RK-45 and DASSL outputs. A correlation coefficient of 1.0 indicates that the two techniques detect level-crossings at the exact same discrete time instants.

Table IV gives the correlation coefficients relating the discrete time instants, for level crossings, generated from the proposed technique with other simulation techniques. As we can see, QSS-1, from Ptolemy, and DASSL from OpenModelica, detect the level-crossings at the same time as the proposed technique. However, Ptolemy's RK-45 integration technique combined with level-crossing detection is less correlated with the proposed technique. RK-45 integration takes fewer number of steps, than QSS-1 and DASSL, and hence, timing errors accumulate during simulation, which results in under or over-estimating the discrete time points for level-crossings. The output traces of the proposed technique and RK-45 can be much more closely related by reducing the maximum Δt . However, doing so would increase the number of integration steps in RK-45. The proposed technique gives an ideal trade-off between the number of integration/simulation steps vs. accuracy.

VI. CONCLUSION AND FUTURE WORK

Hybrid Automata (HA) is a formal approach for specification and validation of safety critical controllers. Simulation of HA is challenging, because of sudden discontinuities caused by level crossings that need to be correctly detected. The current state-of-the-art level crossing detection techniques can potentially miss detecting the level crossing leading to incorrect behaviour.

In this work we propose a new formalism called Quantized State Hybrid Automata (QSHA) and an associated discrete

event simulation framework, which guarantees semantics preserving program behaviour. The primary idea is to select discrete simulation steps based on a *dynamic* quantum in any location of the QSHA. The resultant simulation framework has been proven to always make progress and converge to the first level crossing. Interestingly the dynamic quantum based discrete event simulation approach is quite efficient, outperforming Quantized State System (QSS)-1, Runge-Kutta (RK)-45, and Differential Algebraic System Solver (DASSL) based integration techniques combined with state-of-the-art level crossing detectors.

The current approach syntactically composes a network of Hybrid Automatas (HAs) into a single QSHA before simulation. This approach is known to result in state space explosion. In this future we plan to address this shortcoming by developing a modular discrete event simulation framework, which can simulate each HA in the network individually.

REFERENCES

- [1] A. De Luca, G. Oriolo, and C. Samson, "Feedback control of a nonholonomic car-like robot," in *Robot motion planning and control*. Springer, 1998, pp. 171–253.
- [2] T. A. Henzinger, P. W. Kopke, A. Puri, and P. Varaiya, "What's decidable about hybrid automata?" *Journal of Computer and System Sciences*, vol. 57, no. 1, pp. 94–124, 1998.
- [3] D. Xie, W. Xiong, L. Bu, and X. Li, "Deriving unbounded reachability proof of linear hybrid automata during bounded checking procedure," *IEEE Transactions on Computers*, vol. 66, no. 3, pp. 416–430, 2017.
- [4] M. Tiller, *Introduction to physical modeling with Modelica*. Springer Science & Business Media, 2012, vol. 615.
- [5] S. Matlab, "The Mathworks," 1993.
- [6] F. Zhang, M. Yeddanapudi, and P. J. Mosterman, "Zero-crossing location and detection algorithms for hybrid system simulation," *IFAC Proceedings Volumes*, vol. 41, no. 2, pp. 7967–7972, 2008.
- [7] P. Fritzson, P. Aronsson, A. Pop, H. Lundvall, K. Nyström, L. Saldamli, D. Broman, and A. Sandholm, "Openmodelica-a free open-source environment for system modeling, simulation, and teaching," in *Computer Aided Control System Design, 2006 IEEE International Conference on Control Applications, 2006 IEEE International Symposium on Intelligent Control, 2006 IEEE*. IEEE, 2006, pp. 1588–1595.
- [8] T. Park and P. I. Barton, "State event location in differential-algebraic models," *ACM Transactions on Modeling and Computer Simulation (TOMACS)*, vol. 6, no. 2, pp. 137–165, 1996.
- [9] J. M. Esposito, V. Kumar, and G. J. Pappas, "Accurate event detection for simulating hybrid systems," in *International Workshop on Hybrid Systems: Computation and Control*. Springer, 2001, pp. 204–217.
- [10] E. Kofman, "Discrete event simulation of hybrid systems," *SIAM Journal on Scientific Computing*, vol. 25, no. 5, pp. 1771–1797, 2004.
- [11] E. Kofman and S. Junco, "Quantized-state systems: a devs approach for continuous system simulation," *Trans of the Society for Modeling and Simulation International*, vol. 18, no. 3, pp. 123–132, 2001.
- [12] E. Kofman, "A second-order approximation for devs simulation of continuous systems," *Simulation*, vol. 78, no. 2, pp. 76–89, 2002.
- [13] —, "A third order discrete event method for continuous system simulation," *Latin American applied research*, vol. 36, no. 2, pp. 101–108, 2006.
- [14] X. Floros, F. Bergero, F. E. Cellier, and E. Kofman, "Automated simulation of modelica models with qss methods: The discontinuous case," in *Proceedings of the 8th International Modelica Conference; March 20th-22nd; Technical University; Dresden; Germany*, no. 063. Linköping University Electronic Press, 2011, pp. 657–667.
- [15] F. Bergero, X. Floros, J. Fernández, E. Kofman, and F. E. Cellier, "Simulating modelica models with a stand-alone quantized state systems solver," in *Proceedings of the 9th International MODELICA Conference; September 3-5; 2012; Munich; Germany*, no. 076. Linköping University Electronic Press, 2012, pp. 237–246.
- [16] F. Di Pietro, G. Migoni, and E. Kofman, "Improving a linearly implicit quantized state system method," in *Proceedings of the 2016 Winter Simulation Conference*. IEEE Press, 2016, pp. 1084–1095.

- [17] E. A. Lee, M. Niknami, T. Noudui, and M. Wetter, "Modeling and simulating cyber-physical systems using cyphysim*," in *EMSOFT*, October 2015. [Online]. Available: <http://chess.eecs.berkeley.edu/pubs/1108.html>
- [18] R. Alur, C. Courcoubetis, T. A. Henzinger, and P.-H. Ho, "Hybrid Automata: An Algorithmic Approach to the Specification and Verification of Hybrid Systems," in *Hybrid Systems*. London, UK: Springer-Verlag, 1993, pp. 209–229. [Online]. Available: <http://dl.acm.org/citation.cfm?id=646874.709849>
- [19] D. Curtiss, "Recent extensions of descartes' rule of signs," *Annals of Mathematics*, pp. 251–278, 1918.
- [20] P. Ye, E. Entcheva, S. Smolka, and R. Grosu, "Modelling excitable cells using cycle-linear hybrid automata," *IET systems biology*, vol. 2, no. 1, pp. 24–32, 2008.
- [21] R. Alur, C. Courcoubetis, N. Halbwachs, T. A. Henzinger, P.-H. Ho, X. Nicollin, A. Olivero, J. Sifakis, and S. Yovine, "The algorithmic analysis of hybrid systems," *Theoretical computer science*, vol. 138, no. 1, pp. 3–34, 1995.
- [22] R. Grosu, G. Batt, F. H. Fenton, J. Glimm, C. Le Guernic, S. A. Smolka, and E. Bartocci, "From cardiac cells to genetic regulatory networks," in *International Conference on Computer Aided Verification*. Springer, 2011, pp. 396–411.
- [23] M. S. Jaffe, N. G. Leveson, M. P. E. Heimdahl, and B. E. Melhart, "Software requirements analysis for real-time process-control systems," *IEEE transactions on software engineering*, vol. 17, no. 3, pp. 241–258, 1991.
- [24] "Benchmarks," <https://github.com/amal029/eha>, last accessed - 28.03.2018.
- [25] C. Ptolemaeus, *System Design, Modeling, and Simulation: Using Ptolemy II*. Ptolemy. org, 2014.



Avinash Malik is a senior lecturer at the University of Auckland, New Zealand. His main research interest lies in programming languages for multicore and distributed systems and their formal semantics and compilation. He has worked at organisations such as INRIA in France, Trinity College Dublin, IBM research Ireland, and IBM Watson on the design and the compilation of programming languages. He holds B.E. and Ph.D degrees from the University of Auckland.



Partha S. Roop received his Ph.D degree in computer science (software engineering) from the University of New South Wales, Sydney, Australia, in 2001. He is currently an Associate Professor and is the Director of the Computer Systems Engineering Program with the Department of Electrical and Computer Engineering, the University of Auckland, New Zealand. Partha is an associated team member of the SPADES team INRIA, Rhone-Alpes, France, and held a visiting position in CAU Kiel, Germany, and Iowa State University, USA. His research interests include the design and verification of embedded systems. In particular, he is developing techniques for the design of embedded applications in automotive, robotics, and intelligent transportation systems that meet functional-safety standards.